

Instabilities and oscillations in coagulation equations with kernels of homogeneity one

Michael Herrmann*

Barbara Niethammer†

Juan J.L. Velázquez†

August 6, 2016

Abstract

We discuss the long-time behaviour of solutions to Smoluchowski's coagulation equation with kernels of homogeneity one, combining formal asymptotics, heuristic arguments based on linearization, and numerical simulations. The case of what we call diagonally dominant kernels is particularly interesting. Here one expects that the long-time behaviour is, after a suitable change of variables, the same as for the Burgers equation. However, for kernels that are close to the diagonal one we obtain instability of both, constant solutions and traveling waves and in general no convergence to N -waves for integrable data. On the other hand, for kernels not close to the diagonal one these structures are stable, but the traveling waves have strong oscillations. This has implications on the approach towards an N -wave for integrable data, which is also characterized by strong oscillations near the shock front.

Keywords: Smoluchowski's coagulation equation, kernels with homogeneity one

1 Introduction

Smoluchowski's coagulation equation. In 1916 Smoluchowski derived a mean-field equation to describe coagulation in homogeneous gold solutions, which is nowadays used in a large variety of mass aggregation phenomena [26]. It applies to a homogeneous dilute system of clusters that can coagulate by binary collisions to form larger clusters. If $f(t, \xi)$ denotes the number density of clusters of size $\xi > 0$ at time t , then f satisfies

$$\partial_t f(t, \xi) = \frac{1}{2} \int_0^\xi K(\xi - \eta, \eta) f(t, \xi - \eta) f(t, \eta) d\eta - f(t, \xi) \int_0^\infty K(\xi, \eta) f(t, \eta) d\eta, \quad (1)$$

where the so-called rate kernel K is a nonnegative and symmetric function which describes the microscopic details of the coagulation process.

If clusters are spherical, diffuse by Brownian motion and coagulate quickly when they get within a certain interaction range, Smoluchowski [26] derived the kernel

$$K(\xi, \eta) = (\xi^{1/3} + \eta^{1/3})(\xi^{-1/3} + \eta^{-1/3}).$$

*Westfälische Wilhelms-Universität Münster, Institut für Numerische und Angewandte Mathematik

†Rheinische Friedrich-Wilhelms-Universität Bonn, Institut für Angewandte Mathematik

michael.herrmann@uni-muenster.de, niethammer@iam.uni-bonn.de, velazquez@iam.uni-bonn.de

Further examples of kernels for a diverse range of applications, such as aerosol physics, polymerization, growth of nanostructures, or astronomy, can be found in the survey articles [6, 2, 10]. The well-posedness of the initial value problem corresponding to (1) is by now quite well understood. It is also known that if the kernel K grows too fast at infinity, e.g. if K is homogeneous of degree larger than one, then solutions to (1) exhibit the phenomenon of gelation, that is the loss of mass at finite time, which is linked to the formation of infinitely large clusters. On the other hand, if K has homogeneity smaller than one or if $K(\xi, \eta) \leq C(1 + \xi + \eta)$ and if the initial data have finite mass, then solutions to (1) conserve the mass for all times [14].

A scale invariance of the equation leads to the so-called scaling hypothesis which suggests that the long-time behaviour of solutions to (1) is universal and asymptotically described by self-similar solutions. This issue is so far understood [19] for the two solvable kernels of homogeneity $\gamma \leq 1$, the constant one and the additive one, $K(\xi, \eta) = \xi + \eta$. For these kernels equation (1) can be solved explicitly by Laplace transform. For non-solvable kernels with homogeneity strictly smaller than one, only existence results for self-similar solutions are available [9, 7, 22, 20], while questions about uniqueness and convergence to these self-similar solutions have so far only been answered for a few special cases [15, 20].

Kernels with homogeneity one. Our goal in this article is to investigate the long-time behaviour of solutions to (1) for kernels with homogeneity equal to one. One example is $K(\xi, \eta) = (\xi^{1/3} + \eta^{1/3})^3$ that has been derived for particles moving in a shear flow [26], others appear in gravitational coalescence or charged aerosols [6]. Such kernels represent the borderline case that separates gelation from self-similar coarsening and we expect additional phenomena and technical difficulties. Apart from the solvable additive kernel, for which complete results are available [4, 19], no other kernel of homogeneity one has, at least to our knowledge, been studied in the mathematical literature. Some useful insight into the properties of solutions based on formal considerations has been gained in [28, 16], but not all aspects have been investigated there. It is the goal of this article to provide more information on what to expect on the long-time behaviour of solutions to the coagulation equation with kernels of homogeneity one. We will give some rigorous results for a special case, the diagonal kernel, and provide several conjectures for the general case that we support by numerical simulations.

Self-similar solutions. For the following considerations we rewrite (1) in conservative form, that is as

$$\partial_t(\xi f(t, \xi)) = -\partial_\xi \left(\int_0^\xi d\eta \int_{\xi-\eta}^\infty d\zeta K(\eta, \zeta) \eta f(t, \eta) f(t, \zeta) \right). \quad (2)$$

We are interested in finding self-similar solutions of (2) and hence make the ansatz

$$f(t, \xi) = \frac{1}{s(t)^2} \Phi(x), \quad x = \frac{\xi}{s(t)}. \quad (3)$$

If we plug (3) into (2) we obtain, using that the kernel has homogeneity one, the formulas

$$s(t) = e^{bt}, \quad b > 0, \quad (4)$$

and

$$b(2x\Phi(x) + x^2\Phi'(x)) = \partial_x \left(\int_0^x \int_{x-y}^\infty K(y, z) y \Phi(y) \Phi(z) dz dy \right), \quad (5)$$

which, after integration with respect to x , gives

$$bx^2\Phi(x) = \int_0^x \int_{x-y}^\infty K(y, z) y \Phi(y) \Phi(z) dz dy. \quad (6)$$

A useful change of variables. It turns out that the following change of variables is useful. We define

$$\xi = e^X \quad \text{and} \quad u(t, X) = \xi^2 f(t, \xi) \quad (7)$$

such that (2) becomes

$$\partial_t u = -\partial_X \left(\int_{-\infty}^X \int_{X+\ln(1-e^{Y-X})}^{\infty} K(e^{Y-Z}, 1) u(t, Y) u(t, Z) dZ dY \right). \quad (8)$$

In these new variables, scale invariant solutions correspond to traveling wave solutions. More precisely, if we make the ansatz $u(t, X) = G(X - bt)$, then G must satisfy

$$\begin{aligned} bG(X) &= \int_{-\infty}^X \int_{X+\ln(1-e^{Y-X})}^{\infty} K(e^{Y-Z}, 1) G(Y) G(Z) dZ dY \\ &= \int_{-\infty}^0 \int_{\ln(1-e^Y)}^{\infty} K(e^{Y-Z}, 1) G(Y+X) G(Z+X) dZ dY. \end{aligned} \quad (9)$$

Notice that the translation invariance that we used in the last step in (9) is a consequence of the fact that K has homogeneity one. The relation to the original variables is $\xi^2 f(t, \xi) = G(\ln \xi - bt)$ and $x^2 \Phi(x) = G(X)$, respectively. Furthermore note that the quantity that is preserved by the evolution (1), the first moment of f , now turns into the integral of u , that is $\int_0^\infty \xi f(t, \xi) d\xi = \int_{-\infty}^\infty u(t, X) dX$.

In the following we will only consider traveling waves that can be related to self-similar solutions of (1) which decay sufficiently fast. Therefore, we will restrict ourselves to solutions of (9) which satisfy $G(\infty) = 0$. The precise role of the parameter b will be discussed below, as it depends on the type of kernel as well as on the type of solutions that we will consider.

Class-II kernels. To proceed, we need to distinguish between two types of kernels, a fact that has already been noticed in [28, 16]. In the first case, called class-II kernels in [28], one has $K(\xi, 1) \rightarrow k_0 > 0$ as $\xi \rightarrow 0$. In this case we notice that the integral

$$\int_{-\infty}^X \int_{X+\ln(1-e^{Y-X})}^{\infty} K(e^{Y-Z}, 1) dZ dY$$

is not finite. Consequently, if a solution G to (9) exists for some $b > 0$, then it must at least satisfy $G(X) \rightarrow 0$ as $|X| \rightarrow \infty$.

The most prominent example of a class-II kernel is the additive kernel, for which it is known that there exists a whole family of self-similar solutions with finite mass [19]. One of them has exponential decay, the others decay algebraically such that the second moment is infinite. This family of solutions can be parameterized by the parameter b in (9). In fact, if one normalizes the integral of G to one there is a one-to-one correspondence between b and the decay behaviour of the solutions to (9). The result in [19] provides the existence of self-similar solutions for any $b \geq 2$.

The question whether an analogous result holds for other class-II kernels is presently open. In Section 2 we give self-consistent arguments to describe the expected decay behaviour of self-similar solutions, see the left panel in Figure 1, and formulate a conjecture that self-similar solutions exist for b larger than a critical number b_* that depends on the kernel.

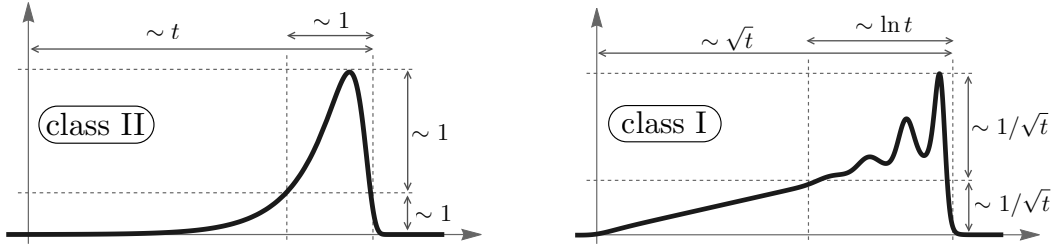


Figure 1: Cartoons of the different long time behavior for data with finite mass. *Left panel:* For class-II kernel we expect to find self-similar solutions, which are transformed into traveling waves by the rescaling (7). *Right panel:* Traveling waves exist also for class-I kernels but carry infinite mass and can exhibit strong oscillations. The long-time behaviour is – at least for some kernels – governed by an N-wave solution with attached traveling wave at the front.

Class-I kernels. We now consider kernels that satisfy $\lim_{x \rightarrow 0} K(x, 1) = 0$ and make the additional assumption, as has been done in [28], that the kernel is asymptotically a power law for small x , that is

$$K(x, 1) \sim c_\alpha x^\alpha \quad \text{as } x \rightarrow 0 \quad \text{for some } \alpha > 0 \text{ and } c_\alpha \geq 0. \quad (10)$$

Such kernels are called class-I kernels in the notation of [28], we sometimes also call such kernels *diagonally dominant*. A limiting case is the diagonal kernel

$$K(x, y) = x^2 \delta_{x-y} \quad (11)$$

for which only particles of the same size are allowed to coagulate. Note that this kernel has homogeneity one since the Dirac distribution has homogeneity minus one. Further examples are given by the following family of kernels (see Figure 2)

$$K_\alpha(x, y) = c_\alpha x^\alpha y^\alpha (x + y)^{1-2\alpha}, \quad \alpha > 0, \quad (12)$$

which interpolates between the additive kernel ($\alpha = 0$) and the diagonal kernel ($\alpha \rightarrow \infty$). Here the constant c_α is a suitable normalization constant that will be chosen later in Section 3.3.

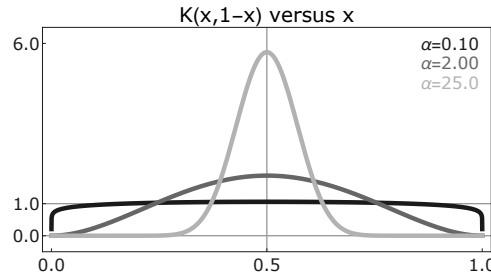


Figure 2: Three kernels of the family in (12) with $c_\alpha = \frac{\Gamma(2+2\alpha)}{\Gamma(1+\alpha)^2}$ such that $\int_0^1 K(x, 1-x) dx = 1$.

In contrast to kernels of class II, for kernels of class I satisfying (10), we have

$$A := \int_{-\infty}^0 \int_{\ln(1-e^Y)}^\infty K(e^{Y-Z}, 1) dZ dY < \infty. \quad (13)$$

Hence, the only self-consistent behaviour of a solution $G(X)$ as $X \rightarrow -\infty$ is $\lim_{X \rightarrow -\infty} G(X) = G(-\infty) = bA^{-1} > 0$. However, then the integral over G is not finite, and this contradicts the

assumption of finite mass, a fact that has already been noticed in [28, 16]. As a consequence, the ansatz (3) is inconsistent. Nevertheless, solutions of (9) are also of interest since they correspond to traveling wave solutions in the variable $\ln \xi$ for $\xi^2 f(t, \xi)$, but they cannot appear as the large time limit for solutions with finite mass. Notice also that here the parameter b determines the asymptotic jump of the traveling wave and can without loss of generality be set equal to one. In Section 3 we first provide an argument based on formal asymptotics that the long-time behaviour of solutions with finite mass is to leading order the same as the long-time behaviour of solutions to the inviscid Burgers equation. As a first step we consider the diagonal kernel in Section 3.2, for which we can show rigorously that solutions converge to an N -wave in the long-time limit. Next, we consider the family of kernels K_α in (12) for different values of α . In Sections 3.3.1 and 3.3.2 we discuss the stability resp. instability of constant solutions before we turn to traveling waves in Section 3.3.3. Numerical simulations suggest that the wave profiles are monotone for large α , i.e. for kernels close to the diagonal one, but oscillatory for small α , a fact that can be explained by a linearization argument. Finally, in Section 3.3.4 we investigate, also numerically, the long-time behaviour of solutions with integrable data. It turns out that, at least for moderate α , the solution converges to an N -wave, but the transition at the shock front is given by a traveling wave and is hence oscillatory for some range of kernels. An illustration is given in the right panel of Figure 1.

2 Class II kernels

Before we consider general class-II kernels, we briefly recall the results on self-similar solutions for the additive kernel, formulated in the variables (7).

2.1 The additive kernel

Proposition 2.1 (Section 6.1 in [19]). *Suppose that $K(\xi, \eta) = \xi + \eta$ and that $b = \frac{1+\rho}{\rho}$. Then there exists for any $\rho \in (0, 1]$ a solution $G_\rho(X)$ to (9) with unit mass, that is $\int_{-\infty}^{\infty} G_\rho(X) dX = 1$. For $\rho = 1$ the solution is*

$$G_1(X) = \frac{1}{\sqrt{2\pi}} e^{\frac{X}{2}} e^{-\frac{e^X}{2}}, \quad (14)$$

while for $\rho \in (0, 1)$ the solution is given by

$$G_\rho(X) = \frac{1}{\pi} \sum_{k=1}^{\infty} \frac{(-1)^{k-1}}{k!} e^{k \frac{\rho}{\rho+1} X} \Gamma\left(1 + k - k \frac{\rho}{1+\rho}\right) \sin\left(k\pi \frac{\rho}{1+\rho}\right). \quad (15)$$

The asymptotics of G for $|X| \rightarrow \infty$ are

$$G_\rho(X) \sim \frac{\sin\left(\frac{\pi\rho}{1+\rho}\right) \Gamma\left(\frac{1}{1+\rho}\right)}{\pi(1+\rho)} e^{\frac{\rho}{1+\rho} X} \quad \text{as } X \rightarrow -\infty \quad (16)$$

and

$$G_\rho(X) \sim \frac{\Gamma(1+\rho) \sin(\pi(1-\rho))}{\pi} e^{-\rho X} \quad \text{as } X \rightarrow \infty. \quad (17)$$

Thus, for any $b \in [2, \infty)$ a self-similar solution with unit mass exists. Notice, that the rescaled function $G_{m,\rho}(X) := m G_\rho(X)$ has mass m and solves (9) with $b = m \frac{1+\rho}{\rho}$.

For the additive kernel it is also easily seen that whenever G satisfies $\int_{-\infty}^{\infty} e^X G(X) dX < \infty$, then it must hold that $\rho = 1$. This follows, since multiplying (9) by e^X and integrating gives $\frac{\rho+1}{\rho} M_2 = 2M_1 M_2 = 2M_2$, where we use the notation $M_i = \int_{-\infty}^{\infty} e^{(i-1)X} G(X) dX$. (These quantities correspond to the i -th moments of $\Phi(x)$).

2.2 Nonsolvable class II kernels

We now assume that K is a general kernel of homogeneity one that satisfies $\lim_{\xi \rightarrow 0} K(\xi, 1) = k_0 > 0$. Without loss of generality we assume in the following $k_0 = 1$.

Heuristics of asymptotic behaviour. We first show that, if a solution G_ρ to (9) exists that satisfies $G_\rho(X) \sim e^{-\rho X}$ as $X \rightarrow \infty$, then necessarily $b = \frac{\rho+1}{\rho}$. (Notice that in general we obtain the relation $b = k_0 \frac{1+\rho}{\rho}$). For that purpose we split the integral

$$\int_{-\infty}^X \int_{X+\ln(1-e^{Y-X})}^{\infty} dZ dY = \int_{-\infty}^X \int_X^{\infty} dZ dY + \int_{-\infty}^X \int_{X+\ln(1-e^{Y-X})}^X dZ dY.$$

Since $K(\xi, 1) \approx 1$ for small ξ and if $G_\rho(X) \sim e^{-\rho X}$ as $X \rightarrow \infty$, then (recall that $\int_{-\infty}^{\infty} G(X) dX = 1$)

$$\int_{-\infty}^X \int_X^{\infty} K(e^{Y-Z}, 1) G_\rho(Y) G_\rho(Z) \approx \int_{-\infty}^X G_\rho(Y) dY \int_X^{\infty} G_\rho(Z) dZ \approx \frac{1}{\rho} e^{-\rho X}$$

as $X \rightarrow \infty$. Furthermore, changing the order of integration,

$$\begin{aligned} \int_{-\infty}^X \int_{X+\ln(1-e^{Y-X})}^{\infty} K(e^{Y-Z}, 1) G_\rho(Y) G_\rho(Z) dZ dY \\ = \int_{-\infty}^X G_\rho(Z) \int_{X+\ln(1-e^{Z-X})}^X K(e^{Y-Z}, 1) G_\rho(Y) dY dZ \\ \approx G_\rho(X) \int_{-\infty}^X G_\rho(Z) \int_{X+\ln(1-e^{Z-X})}^X K(e^{Y-Z}, 1) dY dZ \\ \approx G_\rho(X) = e^{-\rho X} \quad \text{as } X \rightarrow \infty. \end{aligned}$$

Here we used that

$$\int_{X+\ln(1-e^{Z-X})}^X K(e^{Y-Z}, 1) dY = \int_{x-z}^x \frac{1}{y} K\left(\frac{y}{z}, 1\right) dy = \frac{1}{z} \int_{x-z}^x K\left(1, \frac{z}{y}\right) dy \approx \frac{1}{z} \int_{x-z}^x dy = 1.$$

As a consequence, $b = \frac{1+\rho}{\rho}$ if such a solution exists.

Now assume that $G_\rho(X) \sim e^{aX}$ as $X \rightarrow -\infty$. Then, as above,

$$\int_{-\infty}^X \int_X^{\infty} K(e^{Y-Z}, 1) G_\rho(Y) G_\rho(Z) \approx \int_{-\infty}^X G_\rho(Y) dY \int_X^{\infty} G_\rho(Z) dZ \approx \frac{1}{z} e^{-aX} \sim \frac{1}{a} e^{aX}$$

as $X \rightarrow -\infty$. The term $\int_{-\infty}^X \int_{X+\ln(1-e^{Y-X})}^X K(e^{Y-Z}, 1) G_\rho(Y) G_\rho(Z) dZ dY$ give in this case a contribution of higher order. Hence, we have that $a = \frac{\rho}{1+\rho}$.

Thus, we see that if solutions for a given $b > 0$ exist and if they have some exponential behaviour as $X \rightarrow \pm\infty$, then the relation between b and the exponents is the same as in the case of the additive kernel.

Conjecture on existence of solutions. For a general class-II kernel K , we conjecture that there is a critical $\rho_* \in (0, \infty]$, depending on K , such that for any $\rho \in (0, \rho_*)$ there exists a solution G_ρ to (9) that satisfies for $\rho \in (0, \rho_*)$ that $G_\rho(X) \sim e^{-\rho X}$ as $X \rightarrow \infty$, while for $\rho = \rho_*$ it decays double exponentially. If $\rho_* < \infty$ we furthermore conjecture, that there exists $\rho_{**} \geq \rho_*$ such that there is no nonnegative solution to (9) for $\rho > \rho_{**}$.

Notice that the 'fat-tail' solutions for $\rho < \rho_*$ are different from the self-similar solutions with fat tails for kernels with homogeneity $\gamma < 1$. In the latter case, if $\gamma \geq 0$ and some structural assumptions on the kernel are satisfied, there exist self-similar solutions [22, 21] of the form $f(t, \xi) = t^r F(\xi t^{-s})$ with $F(z) \sim z^{-(1+\rho)}$ with $\rho \in (\gamma, 1)$, $s = \frac{1}{\rho-\gamma}$ and $r = 1 + (1 + \gamma)s$. Hence $f(t, \xi) \sim A \xi^{-(1+\rho)}$ as $\xi \rightarrow \infty$ with a time-independent constant A . In contrast to that, consider self-similar solutions for class II kernels with homogeneity one with a profile that decays as $x^{-(2+\rho)}$. Such solutions have time dependent tails of the form $A(t)x^{-(2+\rho)}$ with $A(t) = e^{M_1(1+\rho)t}$, where M_1 denotes the mass. As a consequence, we expect that any existence proof of such solutions should be different from the ones that exist for 'stationary' fat tails.

We conclude this section by a justification of our conjecture that the critical ρ_* is in general not equal to one, but rather depends on the details of the kernel. For that purpose we consider a kernel that is a perturbation of the additive one and look for solutions that are perturbations of the explicit solution of the additive kernel for $b = 2$, given in (14). We will see that in general this perturbation will have a polynomial decay if we fix $b = 2$. In order to get exponential decay it is therefore necessary to change b as well, which leads to a critical value ρ_* that is different from one and possibly even infinity.

For the corresponding computations it is more convenient to go back to the original self-similar variable x . This will allow us to obtain the properties of the solution to the linearized problem by using the Laplace transform. We are looking for solutions of (6) where $K = K_\varepsilon$ is a perturbation of the additive kernel,

$$K_\varepsilon(x, y) = x + y + \varepsilon W(x, y), \quad (18)$$

where W has homogeneity one. We assume that W is smooth and has compact support. We linearize around the explicit solution for $\rho = 1$ for the additive kernel

$$\bar{\Phi}(x) = \frac{1}{\sqrt{2\pi}} x^{-3/2} e^{-\frac{x}{2}}, \quad (19)$$

that is we make the ansatz

$$\Phi(x) = \bar{\Phi}(x) + \varphi(x) \quad \text{with} \quad \int_0^\infty x \varphi(x) dx = 0. \quad (20)$$

If we plug (20) into (6) with $b = 2 + \mu\varepsilon$ and neglect higher order terms, we find the linear equation for φ ,

$$\begin{aligned} 2x^2 \varphi(x) = & \int_0^x \int_{x-y}^\infty y(z+y) (\bar{\Phi}(y)\varphi(z) + \bar{\Phi}(z)\varphi(y)) dz dy \\ & + \varepsilon \int_0^x \int_{x-y}^\infty y W(y, z) \bar{\Phi}(y) \bar{\Phi}(z) dz dy - \mu\varepsilon x^2 \bar{\Phi}(x), \end{aligned} \quad (21)$$

where the second line of (21) contains the source terms.

Since $\bar{\Phi}$ is not integrable, we expect that the same is true for φ and hence that its Laplace transform at zero is not defined. Instead, we introduce

$$\tilde{\varphi}(p) = \int_0^\infty (1 - e^{-pz}) \varphi(z) dz, \quad (22)$$

multiply (21) with e^{-px} and integrate. We call $U(p) = \int_0^\infty (1 - e^{-pz}) \bar{\Phi}(z) dz$ and notice, that the properties of $\bar{\Phi}$ imply that $U(0) = 0$ and $\frac{d}{dp} U(0) = 1$. We obtain

$$\left(\frac{U(p)}{p} - 2 \right) \frac{d^2}{dp^2} \tilde{\varphi}(p) = -\frac{1}{p} \frac{d}{dp} \tilde{\varphi}(p) - \frac{1}{p} \frac{d^2}{dp^2} U(p) \tilde{\varphi} + \tilde{\lambda}(p) + \mu\varepsilon \frac{d^2}{dp^2} U(p), \quad (23)$$

where $\tilde{\lambda}$ contains the transforms of the source terms coming from W . As $p \rightarrow 0$ we obtain to leading order, since $U(p) \sim p$ as $p \rightarrow 0$, that

$$\frac{d^2}{dp^2}\tilde{\varphi} - \frac{1}{p}\frac{d}{dp}\tilde{\varphi} + \frac{\kappa}{p}\tilde{\varphi} = \tilde{\lambda}(0) + \mu\varepsilon\kappa, \quad (24)$$

where $\kappa := \frac{d^2}{dp^2}U(0)$. The solution of (24) behaves as $\tilde{\varphi} \sim p^2 \ln p$ as $p \rightarrow 0$, which corresponds to $\varphi(x) \sim x^{-3}$ as $x \rightarrow \infty$. Hence, in order to obtain an exponentially decaying solution, one needs in general to choose μ different from zero in order to cancel this slow decay behaviour. This indicates that the critical value ρ_* is not necessarily equal to one as in the case of the additive kernel, and is determined by an eigenvalue problem, which is to find the critical b in (9) that yields fast decay of the solution. It remains a challenging task to determine this critical b , at least for general kernels that are not perturbations of the solvable one.

3 Class-I kernels

3.1 Heuristics

We have seen in the Introduction that for class-I kernels there are no self-similar solutions with finite mass. In order to understand what happens to a solution with finite mass in the long time limit, it is convenient to look at the formulation (8). Together with the requirement that the integral of u is finite, it suggests to consider the rescaled function $u_\varepsilon(\tau, \tilde{X}) = \frac{1}{\varepsilon}u(\frac{\tau}{\varepsilon^2}, \frac{\tilde{X}}{\varepsilon})$, where $0 < \varepsilon \ll 1$ is a scaling parameter. This yields

$$\begin{aligned} \partial_\tau u_\varepsilon &= -\partial_{\tilde{X}} \left(\frac{1}{\varepsilon^2} \int_{-\infty}^{\tilde{X}} \int_{\tilde{X} + \varepsilon \ln(1 - e^{-\frac{Y-Z}{\varepsilon}})}^{\infty} K(e^{\frac{Y-Z}{\varepsilon}}, 1) u_\varepsilon(Y) u_\varepsilon(Z) dZ dY \right) \\ &= -\partial_{\tilde{X}} \left(\frac{1}{\varepsilon^2} \int_{-\infty}^0 \int_{\varepsilon \ln(1 - e^{-\frac{Y}{\varepsilon}})}^{\infty} K(e^{\frac{Y-Z}{\varepsilon}}, 1) u_\varepsilon(\tilde{X} + Y) u_\varepsilon(\tilde{X} + Z) dZ dY \right) \\ &\approx -c_0 \partial_{\tilde{X}} (u_\varepsilon(\tilde{X})^2) \end{aligned} \quad (25)$$

and we conclude that u_ε approximately solves the Burgers equation. In (25) we used in the last step that for any continuous function φ with compact support we have

$$\begin{aligned} \int_{-\infty}^0 \int_{\varepsilon \ln(1 - e^{-\frac{Y}{\varepsilon}})}^{\infty} \frac{K(e^{\frac{Y-Z}{\varepsilon}}, 1)}{\varepsilon^2} \varphi(Y) \varphi(Z) dZ dY \\ = \int_{-\infty}^0 \int_{\ln(1 - e^{-Y})}^{\infty} K(e^{y-z}, 1) \varphi(\varepsilon y) \varphi(\varepsilon z) dy dz \rightarrow c_0 \varphi^2(0) \end{aligned}$$

as $\varepsilon \rightarrow 0$ where $c_0 = \int_{-\infty}^0 \int_{\ln(1 - e^{-Y})}^{\infty} K(e^{y-z}, 1) dy dz < \infty$. In other words, on the domain of integration $\{Y < 0, Z > \varepsilon \ln(1 - e^{-\frac{Y}{\varepsilon}})\}$ the rescaled kernels $\varepsilon^{-2}K(e^{\frac{Y-Z}{\varepsilon}}, 1)$ converge to a multiple of a Dirac distribution. Of course, it is far from obvious that u_ε is sufficiently smooth such that the previous argument applies and that hence the long-time behaviour of finite mass solutions should be the same as for the Burgers equation. It is even less obvious that solutions to the coagulation equation provide an approximation to solutions of the Burgers equation that yield entropy solutions in the limit.

Before we are going to discuss several aspects of solutions of the coagulation equation for K_α as in (12) and present corresponding simulations in Section 3.3, we will first consider in Section 3.2 the special case of the diagonal kernel with homogeneity one. In this case one can describe the long-time behaviour of solutions rigorously.

3.2 The diagonal kernel

The diagonal kernel with homogeneity one is given by (11) for which (1) reduces to $\partial_t f(t, \xi) = (\xi/2)^2 f(t, \xi/2)^2 - \xi^2 f(t, \xi)^2$. In this case it is more convenient to introduce the new variables via $x = 2^X$ and rescale time by $\ln 2$, such that the equation for $u(t, X) = \xi^2 f(t/\ln 2, \xi)$ reads

$$\partial_t u(t, X) = u(t, X-1)^2 - u(t, X)^2. \quad (26)$$

Hence the evolution in a point X depends only on the evolution of the discrete values $X-j$ with $j \in \mathbb{N}$. We consider first the infinite system

$$\dot{u}_j(t) = u_{j-1}^2(t) - u_j^2(t), \quad j \in \mathbb{Z}, \quad (27)$$

which can also be interpreted as an upwind discretization of the Burgers equation.

Formal asymptotics. Equation (27) has already been analyzed by BenNaim and Krapivsky [3] via formal asymptotics and numerical analysis. They consider two type of data: nonnegative integrable data with unit mass on the one hand and a decreasing step function, connecting the values one and zero, on the other hand. In the second case, they predict convergence of the solution to a monotone traveling wave G which satisfies $G'(z) = G(z-1)^2 - G(z)^2$. G has the property that $G(z) \sim e^{bz}$ as $z \rightarrow -\infty$, while it decreases double exponentially, that is $G(z) \sim 2^z e^{-\gamma 2^z}$ as $z \rightarrow \infty$. Figure 3 shows convergence to the traveling wave for Riemann data.

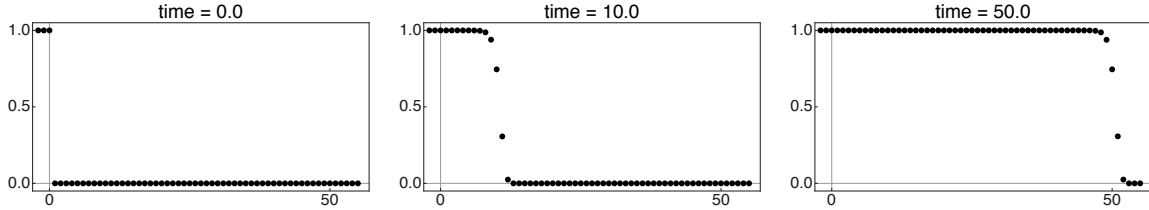


Figure 3: Numerical solution to the Burgers lattice (27) with Riemann initial data: snapshots of $u_j(t)$ for several times t . For $t \rightarrow \infty$ the lattice data approach a monotone travelling wave which propagates with speed 1.

In the case of integrable data, BenNaim and Krapivsky predict that for large times $u_j(t) \sim A_j t^{-1}$ for $0 \leq j \leq j_* = 2\sqrt{t} - 1/4 \ln t$, where $A_j \sim \frac{j}{2} + \frac{\ln j}{4} + O(1)$, that is u_j behaves to leading order as the N -wave with the same mass as the initial data, but there are logarithmic corrections. Furthermore, the behavior at the front j_* is predicted to be given by $u_j(t) \sim \frac{1}{\sqrt{t}} G(j - j_*)$, where G is the traveling wave profile studied before.

We now give the outline of a short proof that establishes convergence to an N -wave of solutions to (27) for summable nonnegative initial data.

Rigorous proof of convergence to an N -wave for the lattice (27). We consider solutions to (27) with initial data (u_j^0) that satisfy

$$u_j^0 \geq 0 \quad \text{for all } j \in \mathbb{Z} \quad \text{and} \quad \sum_{j \in \mathbb{Z}} u_j^0 = M. \quad (28)$$

We introduce the function U_ε as the piecewise constant function given by

$$U_\varepsilon(\tau, x) = \frac{1}{\varepsilon} u_j(t), \quad \text{with } \tau = \varepsilon^2 t \quad \text{and} \quad j = \left\lfloor \frac{x}{\varepsilon} \right\rfloor. \quad (29)$$

Furthermore, we denote by N the continuous nonnegative N -wave with unit mass, that is

$$N(x; M) = \frac{x}{2} \chi_{[0, 2\sqrt{M}]}(x). \quad (30)$$

Proposition 3.1. *We have*

$$\sup_{\tau \in (0, T)} \int_{\mathbb{R}} \left| U_{\varepsilon}(\tau, x) - \frac{1}{\sqrt{\tau}} N\left(\frac{x}{\sqrt{\tau}}; M\right) \right| dx \rightarrow 0 \quad \text{as } \varepsilon \rightarrow 0 \quad (31)$$

or equivalently

$$\sum_j \left| u_j(t) - \frac{1}{\sqrt{t}} N\left(\frac{j}{\sqrt{t}}; M\right) \right| \rightarrow 0 \quad \text{as } t \rightarrow \infty. \quad (32)$$

Proof. We follow the strategy employed, for instance, in [11], where the convergence of different discretization schemes of the Burgers equation is considered. Without loss of generality we assume now $M = 1$. We also note that the maximum principle implies that $u_j(t) \geq 0$ for all $j \in \mathbb{Z}$ and $t > 0$. Furthermore we have $\sum_j u_j(t) = \int U_{\varepsilon}(\tau, x) dx = 1$.

Step 1: (Entropy condition) We first show that

$$(u_{j+1}(t) - u_j(t))_+ \leq \frac{1}{\frac{1}{\sup_j (u_{j+1}^0 - u_j^0)} + t} \quad \text{for all } j \in \mathbb{Z} \quad \text{and } t \geq 0. \quad (33)$$

If we define $w_j := u_{j+1} - u_j$ then w_j satisfies

$$\dot{w}_j = -w_j^2 - w_{j-1}^2 - 2u_j(w_j - w_{j-1})$$

and the statement follows by comparison with the solution of the ODE $y' + y^2 = 0$.

Step 2: (Decay estimate) We establish the temporal decay rate

$$\sup_j u_j(t) \leq \frac{C}{\sqrt{t}}. \quad (34)$$

The main idea is that (33) bounds the increase of u_j in j by $\frac{1}{t}$. Hence, if $\alpha := \max_j u_j(t)$ and k is an index in which the maximum is attained, then u_j is bounded below by the line $\alpha + \frac{j-k}{t}$. Then we have with $k_0 = \lfloor k - \alpha t \rfloor$ that

$$1 \geq \sum_{k_0}^k u_j \geq \sum_{k_0}^k \alpha + \frac{j-k}{t} \geq \alpha^2 t - \sum_{k_0}^k \frac{j-k}{t} \geq \frac{1}{2} \alpha^2 t - C,$$

whence the claim follows.

Step 3: (Compactness in space) We have

$$\frac{d}{dt} \sum_j |u_{j+k} - u_j| \leq 0 \quad \text{for all } k \in \mathbb{Z}, \quad (35)$$

which follows from

$$\begin{aligned} \frac{d}{dt} \sum_j |u_{j+k} - u_j| &= \sum_j \operatorname{sgn}(u_{j+k} - u_j) (-u_{j+k}^2 + u_{j+k-1}^2 + u_j^2 - u_{j-1}^2) \\ &= \sum_j \operatorname{sgn}(u_{j+k} - u_j) ((u_{j+k} + u_j)(u_j - u_{j+k}) + (u_{j+k-1} - u_{j-1})(u_{j+k-1} + u_{j-1})) \\ &\leq -\sum_j |u_{j+k} - u_j| + \sum_j |u_{j+k-1} - u_{j-1}| = 0. \end{aligned}$$

Step 4: (Compactness in time) It holds

$$\sum_j |\dot{u}_j| \leq \frac{2}{c_0 + t}. \quad (36)$$

If we define $J_+ := \{j \in \mathbb{Z} : \dot{u}_j > 0\}$, then by mass conservation $\sum_{j \in J_+} |\dot{u}_j| = \sum_{j \notin J_+} |\dot{u}_j|$. Furthermore (33) implies that $0 \leq u_j - u_{j-1} \leq \frac{1}{c_0 + t}$ for $j \notin J_+$. Hence $\sup_{j \notin J_+} |\dot{u}_j| = \sum_{j \notin J_+} (u_j + u_{j-1})(u_j - u_{j-1}) \leq \frac{C}{c_0 + t}$.

Step 5: (Tightness) As in [11] we conclude that $U_\varepsilon(\tau, \cdot)$ is tight, more precisely that

$$\int_{|x| \geq 2R} U_\varepsilon(\tau, x) dx \leq \int_{|x| \geq R} U_\varepsilon(0, x) dx + \frac{C\sqrt{t}}{R}. \quad (37)$$

Indeed, if $\rho: \mathbb{R} \rightarrow [0, 1]$ is a smooth cut-off function, with the properties that $\rho(x) = 1$ for $x \geq 2$, $\rho(x) = 0$ for $x \leq 1$ and $\rho'(x) \leq 1$, then we can estimate

$$\begin{aligned} \frac{d}{dt} \int_R^\infty U_\varepsilon(t, x) \rho\left(\frac{x}{R}\right) dx &= \int_R^\infty U_\varepsilon(t, x)^2 \frac{\rho\left(\frac{x+\varepsilon}{R}\right) - \rho\left(\frac{x}{R}\right)}{\varepsilon} dx \\ &\leq \frac{C}{R} \int_R^\infty U_\varepsilon(t, x)^2 dx \end{aligned}$$

and (37) thus follows from the bound (34).

Step 6: (A priori estimates for U_ε) The previous steps imply the following a-priori estimates for the rescaled function U_ε . We have the uniform bound $\|U_\varepsilon(\tau, \cdot)\|_{L^\infty(\mathbb{R})} \leq \frac{C}{\sqrt{\tau}}$ by (34), the entropy condition $(\partial_x U_\varepsilon)_+ \leq \frac{1}{\tau}$ follows from (33) and the uniform estimate on the time derivative $\|\partial_\tau U_\varepsilon(\tau, \cdot)\|_{L^1(\mathbb{R})} \leq \frac{C}{\tau}$ is a consequence of (36). Moreover, the equicontinuity

$$\int_{\mathbb{R}} |U_\varepsilon(\tau, x+h) - U_\varepsilon(\tau, x)| dx \leq Ch$$

follows from (35). Finally, (37) provides tightness of U_ε locally uniformly in time.

Step 7: (Compactness and limit equation) These estimates imply, using Riesz-Kolmogorov and Arzela-Ascoli, that the sequence U_ε is precompact in $C([\tau_1, \tau_2]; L^1(\mathbb{R}))$ for arbitrary $0 < \tau_1 < \tau_2 < \infty$. Thus, for a subsequence we have that $U_\varepsilon \rightarrow U$ in $C([\tau_1, \tau_2]; L^1(\mathbb{R}))$ and it follows easily that U is a weak solution of the Burgers equation. In addition it satisfies the same bounds as U_ε , in particular $\partial_x U \leq \frac{C}{t}$ which implies that U is an entropy solution. The tightness estimate also implies $\int_{\mathbb{R}} U(\tau, x) dx = 1$.

Step 8: (Identification of the limit) Using the equation for u_j , the estimate (34) and mass conservation $\sum_j u_j = 1$, we obtain the following weak continuity up to time $\tau = 0$. For $\phi \in C_c^1(\mathbb{R})$

$$\left| \int_{\mathbb{R}} (U_\varepsilon(\tau + h, x) - U_\varepsilon(\tau, x)) \phi(x) dx \right| \leq C \|\phi'\|_{L^\infty} \sqrt{h} \quad \text{for all } \tau > 0.$$

Hence, one can follow the lines of the elementary computations in Step II of the proof of Theorem 1.1 in [11] to conclude that $U(\tau, x) \rightarrow \delta_0$ as $\tau \rightarrow 0$. A key major ingredient to conclude the proof is the uniqueness result for entropy solutions of the Burgers equation with initial data that are measures, provided in [17]. It implies that the limit U is indeed the nonnegative N -wave with unit mass. \square

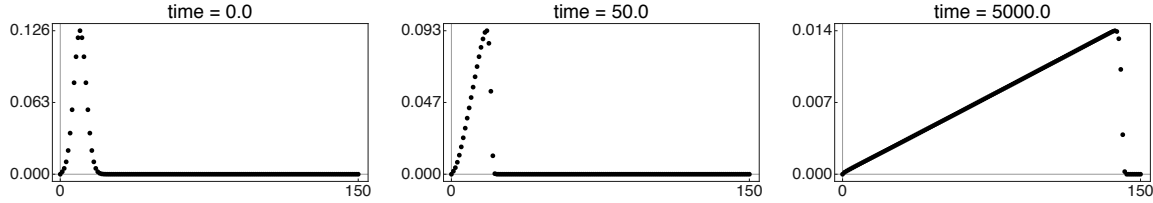


Figure 4: Numerical solution to the Burgers lattice (27) with integrable initial data: For larger times $t \gg 1$, the lattice data resemble an N -wave solution, see Proposition 3.1.

The coagulation equation (26) as a family of lattices (27). As in [15], where the diagonal kernel with homogeneity smaller than one is considered, the analysis of equation (26) can be reduced to the analysis of the functions $\{u(t, n + \theta)\}_{n \in \mathbb{Z}}$ with $\theta \in [0, 1)$. We will call each set of points $\{X_n = n + \theta : n \in \mathbb{Z}\}$ a fibre. The union of all fibres with $\theta \in [0, 1)$ covers the whole real line. In spite of the fact that the dynamics given by independent fibres is easy to describe, it yields interesting oscillatory behaviours and the onset of peak-like solutions in some regions. We have seen that the N -waves defined in (30) depend on the mass contained in each fibre, i.e. on the number $M(\theta) = \sum_{n=-\infty}^{\infty} u(t, n + \theta)$, which is constant in time for each fibre. Proposition 3.1 implies that the values $\{u(t, n + \theta)\}_{n \in \mathbb{Z}}$ behave asymptotically as an N -wave with mass $M(\theta)$, that is

$$u(n + \theta, t) \sim \frac{1}{\sqrt{t}} N\left(\frac{n + \theta}{\sqrt{t}}; M(\theta)\right) \quad \text{as } t \rightarrow \infty. \quad (38)$$

Given that the support of the functions on the right-hand side of (38) depends on θ , it follows that the function $u(t, X)$ increases linearly if $X \in [0, \sqrt{M_{\min} t}]$, where $M_{\min} = \min_{\theta \in [0, 1]} M(\theta)$. On the other hand, if $X > \sqrt{M_{\min} t}$ we might have in each interval in the X variable with length 1 regions where u vanishes and regions where u is of order $\frac{1}{\sqrt{t}}$. If we denote the integer part of a real number $r \in \mathbb{R}$ as $[r]$ and the fractional part as $\text{frac}(r) = r - [r]$. Then (38) implies

$$u(t, X) \sim \frac{1}{\sqrt{t}} N\left(\frac{X}{\sqrt{t}}; M(\text{frac}(X))\right) \quad \text{as } t \rightarrow \infty. \quad (39)$$

Notice that this formula implies oscillatory behaviour in the variable X for $u(t, X)$ if $X > \sqrt{M_{\min} t}$ in the generic case that the function $M(\theta)$ is not constant (see Figure 5 for an illustration).

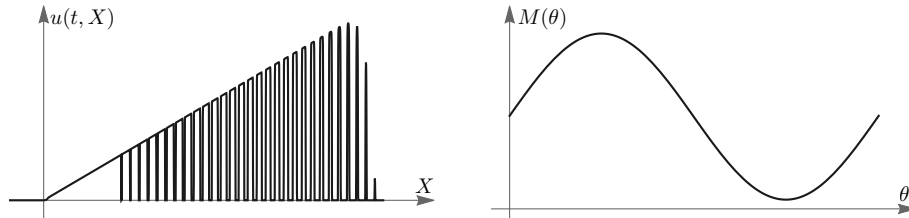


Figure 5: Cartoon of an highly oscillatory solution to the coagulation equation (26) that is composed by a θ -family of N -wave solutions to the lattice (27) with nonconstant mass distribution $M(\theta)$, see (39).

3.3 The general case

In this Section we compare the behaviour of solutions of (1) for kernels from the family K_α as in (12) by means of formal asymptotics and numerical simulations. It turns out that the solutions

of (1) exhibit different features depending on whether α is small, i.e. K_α is close to the additive kernel, or α is large, i.e. K_α is close to the diagonal kernel.

A relevant feature of the case of large α is that the homogeneous solutions are unstable, while they are stable for small α (with a threshold $\alpha_{crit} \approx 35$).

Also the shape of the traveling wave depends sensitively on the size of α . Somewhat counterintuitively to the findings of the stability and instability respectively of the constant solution, for large α the numerical simulations suggest that the traveling wave is monotone, while for small α the traveling wave has oscillations on the left of the front, that become large, when α becomes small. The threshold for oscillations to appear is $\alpha_* \approx 20.1$.

Finally we investigate in Section 3.3.4 the long-time behaviour of solutions with integrable data. For all values of α we observe convergence to an N -wave. However, for small values of α , there are strong oscillations on the left of the shock front (cf. the right picture in Figure 1). This is explained by the expectation that the transition at the shock front is described by a rescaled traveling wave front which we have seen to be oscillatory for small α .

3.3.1 Instability of the constant solution for near-diagonal kernels

Due to the property (13) a constant is a solution of the coagulation equation (8). We examine the stability of this constant solution, that we can without loss of generality assume to be equal to 1. If we plug the ansatz $u = 1 + h(X)$ into (8) we obtain to leading order

$$\partial_t h(X) + \partial_X \left(\int_{-\infty}^0 dY \int_{\ln(1-e^Y)}^{\infty} dZ [K(e^{Y-Z}, 1)(h(Y+X) + h(Z+X))] \right) = 0.$$

We define the Fourier transform of h by $h(X) = \frac{1}{\sqrt{2\pi}} \int_{-\infty}^{\infty} H(k) e^{ikX} dk$ such that

$$\partial_t H(k) = M(k) H(k), \quad (40)$$

with

$$M(k) = -ik \int_{-\infty}^0 dY \int_{\ln(1-e^Y)}^{\infty} dZ [K(e^{Y-Z}, 1)(e^{ikY} + e^{ikZ})]. \quad (41)$$

There are instabilities for particular wave numbers k if $\text{Re}(M(k)) > 0$.

The following result establishes the existence of unstable wave numbers for a broad class of kernels.

Proposition 3.2. *Suppose that K is of the form*

$$K(x, y) = (x + y) \eta \left(\frac{x}{x + y} - \frac{1}{2} \right), \quad (42)$$

where η is a nonnegative, nonzero Radon measure with $\text{supp } \eta(\cdot) \subset [-\varepsilon, \varepsilon]$, $\eta(s) = \eta(-s)$ and $\int_{\mathbb{R}} \eta(s) ds = 1$. Let $M(k)$ be as in (41) and $\varepsilon > 0$ sufficiently small. Then $\text{Re}(M(\frac{2\pi}{\ln 2})) > 0$.

Proof. We can write η as $\eta(x) = \int_{-\frac{1}{2}}^{\frac{1}{2}} \eta(s) \delta(x - s) ds$. Using (41) and (42) we obtain

$$M(k) = - \int_{-\frac{1}{2}}^{\frac{1}{2}} \eta(s) W(k, s) ds, \quad (43)$$

where

$$W(k, s) = ik \int_{-\infty}^0 dY \int_{\ln(1-e^Y)}^{\infty} dZ \left[(e^{Y-Z} + 1) \delta \left(\frac{e^{Y-Z}}{e^{Y-Z} + 1} - \frac{1}{2} - s \right) (e^{ikY} + e^{ikZ}) \right]. \quad (44)$$

The identity $(e^\xi + 1)\delta\left(\frac{e^\xi}{e^\xi + 1} - \frac{1}{2} - s\right) = \frac{(e^\xi + 1)^3}{e^\xi}\delta\left(\xi - \ln\left(\frac{1+2s}{1-2s}\right)\right)$ implies

$$W(k, s) = \frac{8ik}{(1-2s)^2(1+2s)} \int_{-\infty}^0 dY \int_{\ln(1-e^Y)}^{\infty} dZ \left[\delta\left(Y - Z - \ln\left(\frac{1+2s}{1-2s}\right)\right) (e^{ikY} + e^{ikZ}) \right].$$

With $\theta = \ln\left(\frac{1+2s}{1-2s}\right)$ the only values of Y contributing to the integral defining $W(k, s)$ are those with $Y \in [-\ln(1+e^{-\theta}), 0]$ and $Z = Y - \theta$ whence

$$\begin{aligned} W(k, s) &= \frac{8ik}{(1-2s)^2(1+2s)} \int_{-\ln(1+e^{-\theta})}^0 (1 + e^{-ik\theta}) e^{ikY} dY \\ &= \frac{8}{(1-2s)^2(1+2s)} (1 + e^{-ik\theta} - (1 + e^{-\theta})^{-ik} - (1 + e^{\theta})^{-ik}) \\ &= \frac{8}{(1-2s)^2(1+2s)} \left(1 + \left(\frac{1-2s}{1+2s}\right)^{ik} - \left(\frac{1+2s}{2}\right)^{ik} - \left(\frac{1-2s}{2}\right)^{ik} \right). \end{aligned}$$

We take $k = \frac{2\pi}{\ln 2}$. Then, combining the factors $\ln 2$ and using the periodicity of \cos , we find

$$\begin{aligned} \operatorname{Re} W(k_1, \tfrac{1}{2} + s) &= \frac{8}{(1-2s)^2(1+2s)} \left(1 + \cos\left(k_1 \ln\left(\frac{1-2s}{1+2s}\right)\right) \right. \\ &\quad \left. - \cos(k_1 \ln(1+2s)) - \cos(k_1 \ln(1-2s)) \right). \end{aligned}$$

Expanding the function above using Taylor's series we find $\operatorname{Re} W(k_1, \tfrac{1}{2} + s) = -32(k_1 s)^2 + O(s^3)$ as $s \rightarrow 0$, and thus the result follows from (43) if ε is sufficiently small. \square

PDE approximation and convective instabilities It is possible to give an interpretation of this instability of the constant by approximating the coagulation equation (8) by a PDE. Equation (8) with K as in (42) can be rewritten as

$$\begin{aligned} \partial_t u(X) + u(X) \int_{-\infty}^{\infty} \left(\frac{e^Z + 1}{e^Z} \right) \eta\left(\frac{1}{1+e^Z} - \frac{1}{2}\right) u(X+Z) dZ \\ - \int_{-\infty}^0 \frac{1}{(1-e^Y)^2} \eta\left(e^Y - \frac{1}{2}\right) u(X+Y) u(X + \ln(1-e^Y)) dY = 0. \end{aligned}$$

We now use the change of variables $\frac{1}{1+e^Z} - \frac{1}{2} = \frac{\xi}{2}$ in the first integral and $e^Y - \frac{1}{2} = \frac{\xi}{2}$ in the second one. Moreover, we will assume, in order to simplify the numerical constants, that $\eta(s) = \frac{1}{4\varepsilon} \zeta\left(\frac{2s}{\varepsilon}\right)$, $\int \zeta(s) ds = 1$ and $\zeta(s) = \zeta(-s)$. Then

$$\begin{aligned} \partial_t u(X) + u(X) \int_{-1}^1 u\left(X + \ln\left(\frac{1-\xi}{1+\xi}\right)\right) \frac{\frac{1}{\varepsilon} \zeta\left(\frac{\xi}{\varepsilon}\right) d\xi}{(1+\xi)(1-\xi)^2} \\ - \int_{-1}^1 u(X - \ln 2 + \ln(1+\xi)) u(X - \ln 2 + \ln(1-\xi)) \frac{\frac{1}{\varepsilon} \zeta\left(\frac{\xi}{\varepsilon}\right) d\xi}{(1+\xi)(1-\xi)^2} = 0. \end{aligned} \quad (45)$$

We can expand the terms with logarithm in the arguments, using Taylor up to second order. Then (45) can be approximated by

$$\begin{aligned} 0 = \partial_t u(X) + \Lambda_0 \left[u(X)^2 - u(X - \ln 2)^2 \right] \\ + \Lambda_2 \varepsilon^2 \left[-2u(X) \partial_X u(X) + 2u(X) \partial_X^2 u(X) - W(X) \right] \end{aligned} \quad (46)$$

with

$$W(X) = -u(X - \ln 2)\partial_X u(X - \ln 2) + u(X - \ln 2)\partial_X^2 u(X - \ln 2) - (\partial_X u(X - \ln 2))^2$$

and

$$\Lambda_0 = \int_{-1}^1 \eta \frac{\zeta(\eta) d\eta}{(1 + \varepsilon\eta)(1 - \varepsilon\eta)^2}, \quad \Lambda_2 = \int_{-1}^1 \eta^2 \zeta(\eta) d\eta.$$

Notice that $\Lambda_0 \rightarrow 1$ as $\varepsilon \rightarrow 0$. The approximation (46) is valid as long as the characteristic lengths associated to the function u are smaller than ε . This condition holds, for instance, if $|\partial_X u| \ll \frac{u}{\varepsilon}$ and similar conditions for higher order derivatives hold. Equation (46) suggests that the coagulation equation is ill-posed and has the same type of instabilities as backward parabolic equations. However, this is not really so, because the approximation (46) is only valid if the wave numbers k are smaller than $\frac{1}{\varepsilon}$. Nevertheless the type of instabilities exhibited by backward parabolic equations explain the instabilities in Proposition 3.2. Indeed, writing $u(X) = 1 + h(X)$ and linearizing (46) around $u = 1$, we obtain

$$\begin{aligned} \partial_t h(X) + 2\Lambda_0 [h(X) - h(X - \ln 2)] \\ + \Lambda_2 \varepsilon^2 [-2\partial_X h(X) + 2\partial_X^2 h(X) + \partial_X h(X - \ln 2) - \partial_X^2 h(X - \ln 2)] = 0. \end{aligned}$$

Then, the Fourier transform of h , denoted as $H(k)$, satisfies (40) with $M(k)$ approximated as

$$M(k) = -2\Lambda_0(1 - e^{-ik \ln 2}) - \Lambda_2 \varepsilon^2 [-2ik - 2k^2 + ike^{-ik \ln 2} + k^2 e^{-ik \ln 2}] \quad (47)$$

if $k \ll \frac{1}{\varepsilon}$ and thus

$$\text{Re}(M(k)) = -2\Lambda_0(1 - \cos(k \ln 2)) + \Lambda_2 \varepsilon^2 [2k^2 + k \sin(k \ln 2) - k^2 \cos(k \ln 2)]$$

if $k \ll \frac{1}{\varepsilon}$. The terms associated to the diagonal kernel yield the periodic contribution $-2\Lambda_0(1 - \cos(k \ln 2))$ which gives stable behaviour, although neutrally stable for $k = k_n = \frac{2\pi n}{\ln 2}$ with $n \in \mathbb{Z}$. The leading contribution among the terms of order ε for large k is the term $2\Lambda_2 \varepsilon^2 k^2$ which is due to the backward parabolic term $2\Lambda_2 \varepsilon^2 \partial_X^2 h(X)$. The instability induced by this term at the values $k = k_n$ explain the instabilities obtained above. This term becomes of order one if k is of order $\frac{1}{\varepsilon}$.

The linear instability of the homogeneous positive solutions described above is analogous to many instabilities arising in problems of pattern formation (see e.g. [27] or page 16 in [5]), but it does not take place for the standard viscous regularization of the Burgers equation.

If $\bar{k} \in \mathbb{R}$ is one of the values for which $\text{Re}(M_\varepsilon(k)) > 0$ we obtain disturbances of homogeneous solutions of the form

$$\exp(\text{Re}(M(\bar{k}))t) \exp(i(\bar{k}X + \text{Im}(M(\bar{k}))t)). \quad (48)$$

Notice that the approximation (47) allows to approximate $\text{Im}(M(k))$ if k is of order one since $\text{Im}(M(k)) = -2\Lambda_0 \sin(k \ln 2)$ as $\varepsilon \rightarrow 0$. Therefore (48) can be interpreted as a disturbance with wave number \bar{k} propagating towards increasing values of X with velocity $\frac{|\text{Im}(M(\bar{k}))|}{\bar{k}}$. Notice that due to the presence of convective terms a small disturbance that is initially localized at $X = X_0$ with unstable wave numbers can become of order one, due to its exponential growth, at values $X = X_1$ with $X_1 - X_0 \gg 1$. This phenomenon, known as convective instability takes place in many other situations, such as spiral waves in excitable media [25] or plasma physics (see e.g. Chapter 62 of [13]).

3.3.2 Stability of the constant solutions for K_α .

Interestingly, for kernels that are not close to the diagonal one, the constant solution is stable. Here we consider $K_\alpha(x, y)$ as in (12) for different values of α with the normalization

$$c_\alpha = \frac{1}{B(\alpha, \alpha-1)(\psi(2\alpha-1) - \psi(\alpha))}, \quad \text{where } \psi(z) = \frac{\Gamma'(z)}{\Gamma(z)}, \quad B(\alpha, \alpha-1) = \frac{\Gamma(\alpha)\Gamma(\alpha-1)}{\Gamma(2\alpha-1)}. \quad (49)$$

This choice is such that the constant A in (13) satisfies $A = 1$.

We will denote as $M_\alpha(k)$ the function $M(k)$ defined in (41) for the kernels $K_\alpha(x, y)$. Some elementary, but tedious computations yield

$$M_\alpha(k) = -\frac{\Gamma(2\alpha-1)}{\Gamma(\alpha)(\psi(2\alpha-1) - \psi(\alpha))} \left[\frac{\Gamma(\alpha)}{\Gamma(2\alpha-1)} - \frac{\Gamma(\alpha+ik)}{\Gamma(2\alpha+ik-1)} \right] - \frac{\Gamma(2\alpha-1)\Gamma(\alpha+ik-1)}{\Gamma(\alpha)\Gamma(\alpha-1)(\psi(2\alpha-1) - \psi(\alpha))} \left[\frac{\Gamma(\alpha-ik)}{\Gamma(2\alpha-1)} - \frac{\Gamma(\alpha)}{\Gamma(2\alpha+ik-1)} \right] \quad (50)$$

We have plotted the function $k \rightarrow \text{Re}(M_\alpha(k))$ for $k \in \mathbb{R}$ for different values of α in Figure 6.

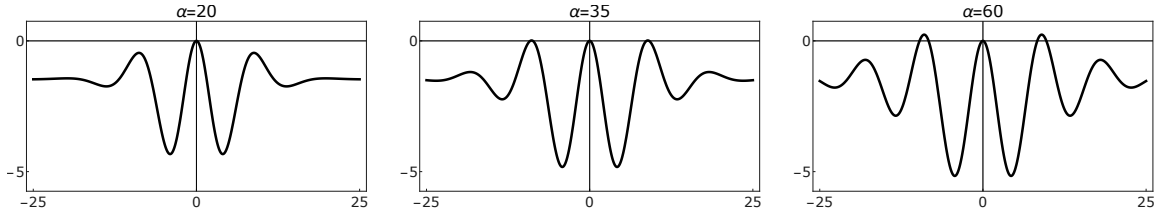


Figure 6: Real part of the function M_α from (50) for three values of α . For $\alpha = \alpha_{\text{crit}} \approx 35$ we observe a change in the stability of the constant solution, see (53).

Notice that for large α we are in an analogous situation to the one discussed in Section 3.3.1 and we can expect to find values $k \in \mathbb{R}$ with $\text{Re}(M_\alpha(k)) > 0$. This can be seen in Figure 6. On the other hand, we can also see that $\text{Re}(M_\alpha(k)) \leq 0$ for smaller values of α . Moreover $\text{Re}(M_\alpha(k)) = 0$ only for $k = 0$. Therefore, the constant solutions are stable for this range of values of α . The computations of $\text{Re}(M_\alpha(k))$ indicate that the critical value of α for which the change of stability takes place is $\alpha_{\text{crit}} = 35$.

In Figure 7 we see the results of numerical simulations of the coagulation equation with initial data that are perturbations of the constant solutions. They confirm that for $\alpha < \alpha_{\text{crit}}$ the perturbations do not grow, while for $\alpha > \alpha_{\text{crit}}$ the perturbation becomes oscillatory and grows.

3.3.3 Traveling wave solutions.

In this section we compare the traveling wave solutions which solve (9) with the kernels $K_\alpha(x, y)$ in (12) for different values α . As mentioned before, we can set without loss of generality $b = 1$. Then, since $A = 1$ we have $G(-\infty) = 1$. Numerical computations of these traveling waves for different values of α can be seen in Figure 8.

These pictures show that the waves separate from the value $G = 1$ at $X = -\infty$ in an oscillatory manner. In order to understand this fact we consider the linearization of (9) near $G(-\infty) = 1$ and write $G = 1 + H(X)$. Then we obtain the following linearized problem

$$H(X) = \int_{-\infty}^0 dY \int_{\ln(1-e^Y)}^{\infty} dZ K(e^{Y-Z}, 1) [H(Y+X) + H(Z+X)]. \quad (51)$$

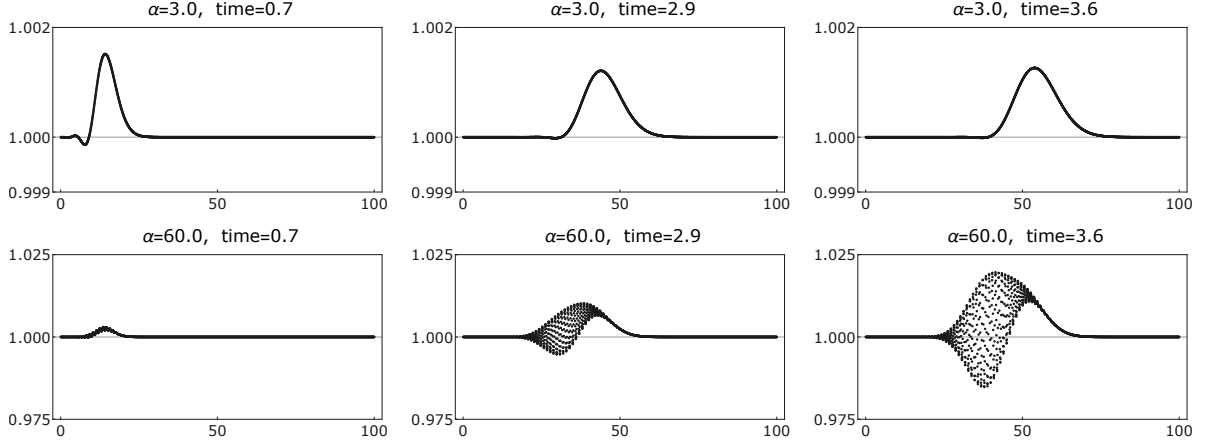


Figure 7: Numerical simulations of the coagulation equation with initial data that are perturbations of a constant for $\alpha = 3.0$ (top) and $\alpha = 60$ (bottom). The numerical scheme as well as the choice of the space and time units are described in the appendix.

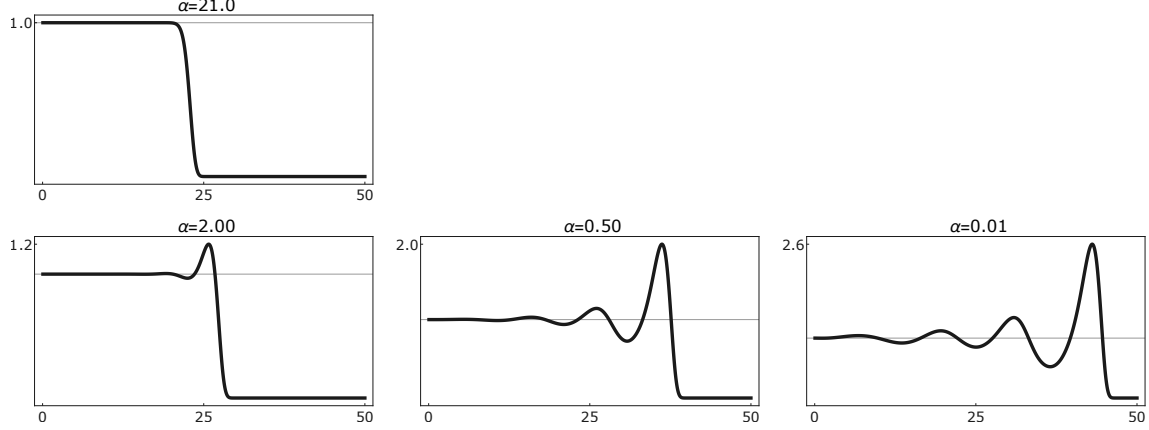


Figure 8: The shape of the traveling wave for different values of α (u against X).

If we look for solutions of (51) of the form $H(X) = e^{i\eta X}$ with $\eta \in \mathbb{C}$ we find $-i\eta = M(\eta)$ with $M(\cdot)$ as in (41).

In order to obtain solutions of (51) which tend to zero as $X \rightarrow -\infty$ we need to obtain solutions of $-i\eta = M(\eta)$ such that $\text{Im}(\eta) < 0$. Oscillatory behaviours arise if the corresponding solution satisfies $\text{Re}(\eta) \neq 0$. Therefore, we might expect to have solutions of (9) oscillating as $X \rightarrow -\infty$ if the roots of $-i\eta = M(\eta)$ with the largest value of $\text{Im}(\eta)$ in the half-plane $\{\eta : \text{Im}(\eta) < 0\}$ satisfy $\text{Re}(\eta) \neq 0$. Thus, if M_α denotes the function $M(\cdot)$ for the kernels K_α in (12) with c_α as in (49) we need to investigate the roots of

$$M_\alpha(k) + ik = 0 \quad (52)$$

in the half plane $\{\text{Im}(k) < 0\}$. These roots are plotted in Figure 9. We can see that, for $\alpha < \alpha_*$, with $\alpha_{\text{crit}} \approx 20$, the roots of (52) in the half-plane $\{\text{Im}(k) < 0\}$ with largest value of $\text{Im}(k)$ have $\text{Re}(k) \neq 0$, while for $\alpha > \alpha_*$ a unique root with $\text{Re}(k) = 0$.

Therefore we expect that $G(X) \rightarrow 1$ as $X \rightarrow -\infty$, with oscillations of decreasing amplitude as $X \rightarrow -\infty$ if $\alpha < \alpha_*$, while G is monotone if $\alpha > \alpha_*$. This scenario is confirmed by direct numerical simulations of the solutions of (8) (cf. Figure 8).

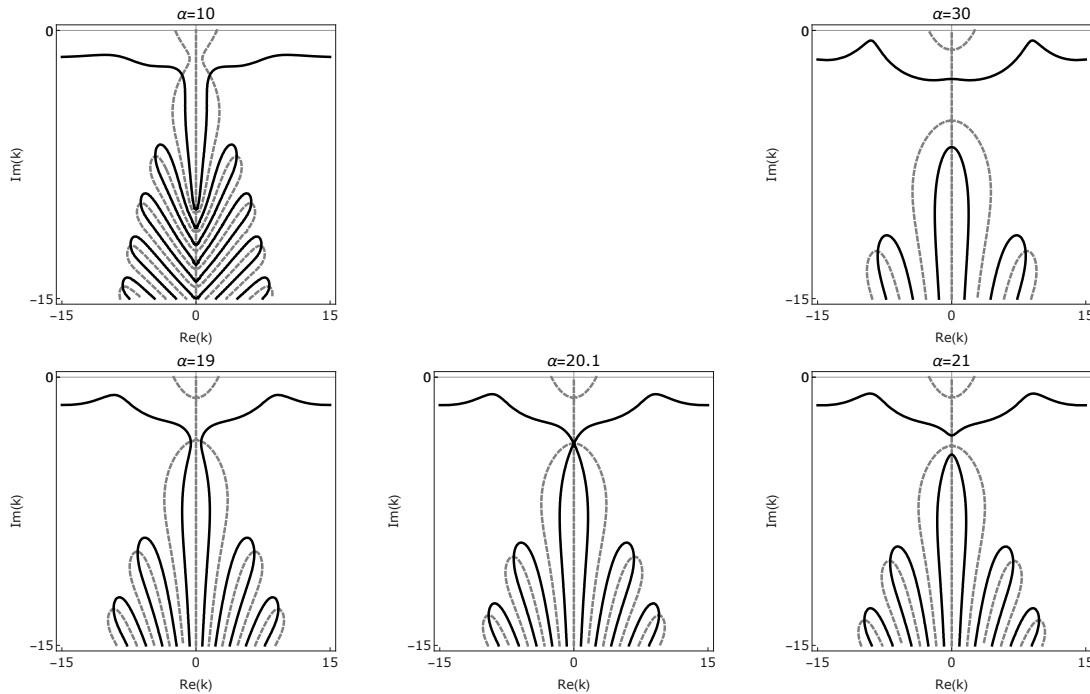


Figure 9: Zeros of $\text{Re}(M_\alpha(k) + ik)$ (black, solid) and $\text{Im}(M_\alpha(k) + ik)$ (gray, dashed) in the complex half plane $\text{Im}(k) < 0$ and for several values of α , see (52). The traveling wave solution for the α -kernel (12) is oscillatory and monotone for $\alpha < \alpha_*$ and $\alpha > \alpha_*$, respectively, where $\alpha_* \approx 20.1$.

Interestingly, since the stability of the constant solution is equivalent to

$$\max_{k \in \mathbb{R}} (\text{Re}(M_\alpha(k))) \leq 0, \quad (53)$$

we see that both, stability of the constant and monotonicity of traveling waves, depend on the same analytic function $M_\alpha(\cdot)$. These conditions are obviously not equivalent. If $\alpha < \alpha_*$ the constant solution is stable, but the traveling wave is oscillatory, while, a bit paradoxically, for $\alpha > \alpha_{\text{crit}}$ the constant solution is unstable for the traveling wave is monotone for $X \rightarrow -\infty$. Only if $\alpha \in (\alpha_*, \alpha_{\text{crit}})$ the constant solution is stable and the traveling is monotone.

Due to the convective instabilities discussed in Section 3.3.1 structures such as traveling waves might only be stable under perturbations that are sufficiently small as $X \rightarrow -\infty$ such that they do not have time to increase before they arrive at the front of the wave. On the other hand the dissipative effects at the front where the values of u decay in lengths of order one, might have stabilizing effects. Therefore, the stability of the fronts for the diagonal kernel suggests that the fronts should be stable also for near-diagonal kernels under perturbations which are still small when they arrive to the back of the front.

Figure 10 shows the result of numerical simulations which indicate the stability of the traveling wave for small α , but shows that the traveling wave is unstable for $\alpha > \alpha_{\text{crit}}$.

In the range $\alpha \in (0, \alpha_*)$ there are no convective instabilities, but the traveling waves connecting the values of $G(-\infty) > 0$ with $G(\infty) = 0$ exhibit strong oscillations and peaks. The numerical simulations of (8) suggest that these waves are nevertheless stable. This is an intriguing feature which deserves a more careful understanding. In a forthcoming paper [23] we will construct via formal matched asymptotic expansions a traveling wave solution for kernels that are similar to K_α for small α . This analysis also yields precise expressions for the size and width of the peaks.

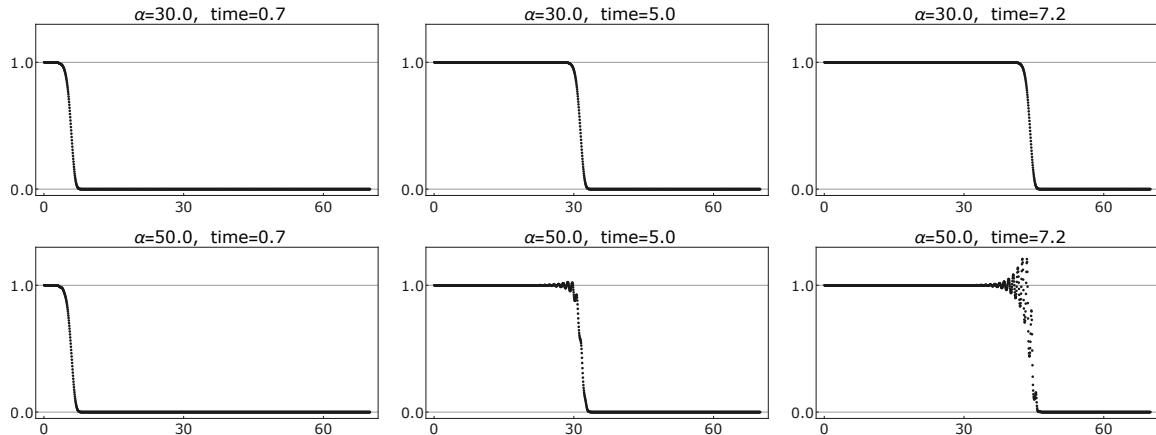


Figure 10: Stability versus instability of the traveling wave for small and large α respectively.

The origin of these oscillations is not clear to us. We have however observed them in other examples, in the construction of self-similar solutions to the coagulation equation with kernel $K(\xi, \eta) = (\xi\eta)^\lambda$ with $\lambda \in (0, 1/2)$ [18]. Also in this case solutions develop oscillations that become more extreme the smaller λ is. Oscillatory traveling waves of similar shape and their stability properties have also been studied in [24], for a generalized KdV-Burgers equation, which contains diffusive and dispersive effects. The effect of the diffusive effects is strong enough to allow the existence of stable traveling waves, but the dispersive effects are relevant yielding highly oscillatory traveling waves. It is natural to ask if the oscillatory behaviour of the traveling waves in the coagulation equation can be explained by a similar competition between diffusive and dispersive effects.

3.3.4 Long-time behaviour of solutions for integrable data.

In the case of solutions of (8) with integrable initial data, the analogies with the classical Burgers equation suggest that solutions of (8) should behave asymptotically as N -waves. Van Dongen and Ernst [28] had already predicted the correct time scale on which a non-trivial limit should appear and also predicted that the transition profile is given as a solution of (9), but the explicit connection to the Burgers equation and N -waves has not been made.

In numerical simulations for K_α with $\alpha < \alpha_{\text{crit}}$ (see Figure 11) we indeed observe convergence to an N -wave. We also see, however, that the approach to the N -wave is quite unusual, at least for small α . In this case, as discussed in Section 3.3.2 the traveling waves connecting the values at the back and rear of the shock appearing in the N -wave exhibit strong oscillations if α is small and have the property that the maximum values of u along these waves are much larger than the values of u on the back of the wave. These strong oscillations are visible in Figure 11. We also conjecture that, as predicted in the case of diagonal kernel by [3], that the transition region scales as $\ln t$ as $t \rightarrow \infty$ (see right panel in Figure 1).

In the case that $\alpha > \alpha_{\text{crit}}$, the same considerations indicated above concerning the stability of the fronts under convective instabilities can be raised about the stability of the N -waves. In the region where the function u is increasing along the N -wave we can assume that the amplitude is approximately constant and then disturbances with wavelength of order one might propagate along the wave and modify in a significant manner the shape of the wave before the disturbances arrive to the region where u decreases. Numerical simulations for smooth data with compact support for large α indicate that this is indeed the case (see Figure 12). The main issue here is

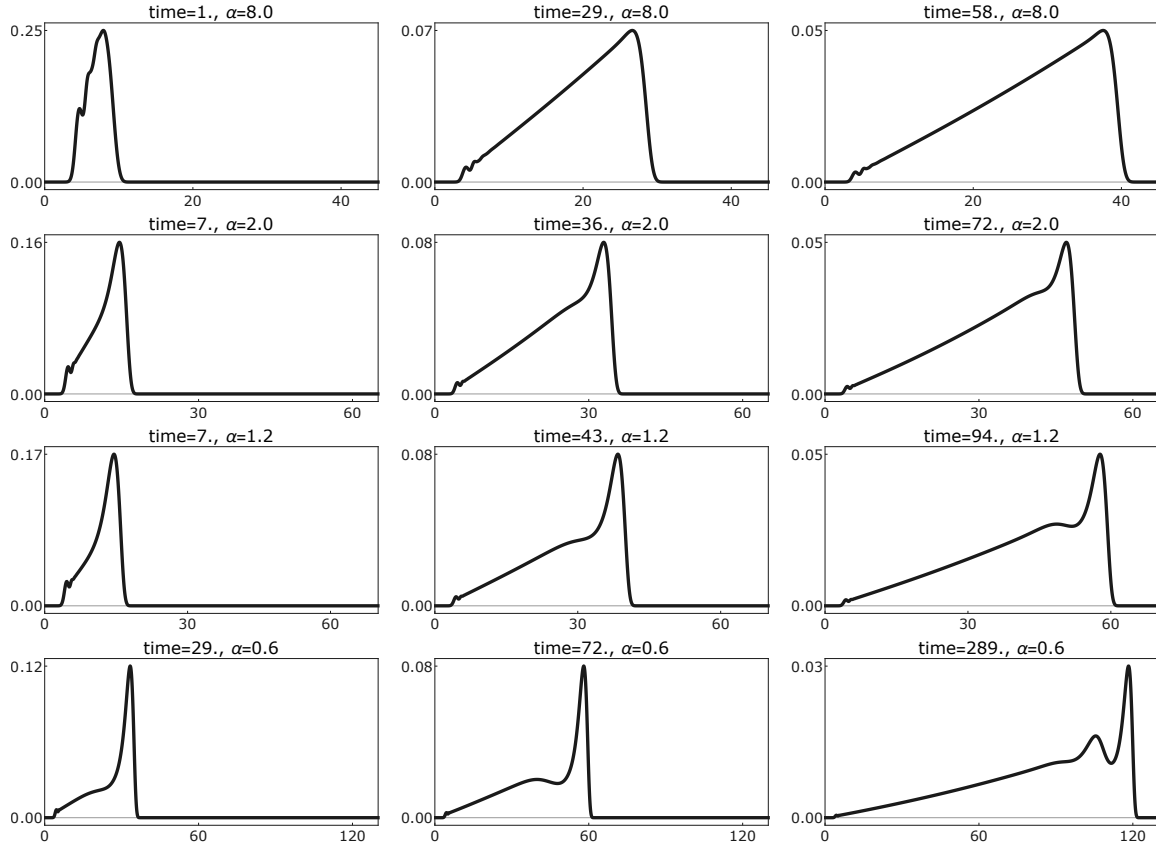


Figure 11: Convergence to the N-wave for $\alpha = 8$ (top), $\alpha = 2$ (second row), $\alpha = 1.2$ (third row) and $\alpha = 0.6$ (bottom).

to estimate the amplitude of the disturbances associated to unstable Fourier wave numbers in regions where X is of order one. We also observe in Figure 12 oscillations at the shock which are reminiscent of the oscillations for the diagonal kernel (see Figure 5) that are due to fibres with different mass. Thus, it will also be relevant to understand the mass exchange between different fibres that takes place for kernels that are close to the diagonal one.

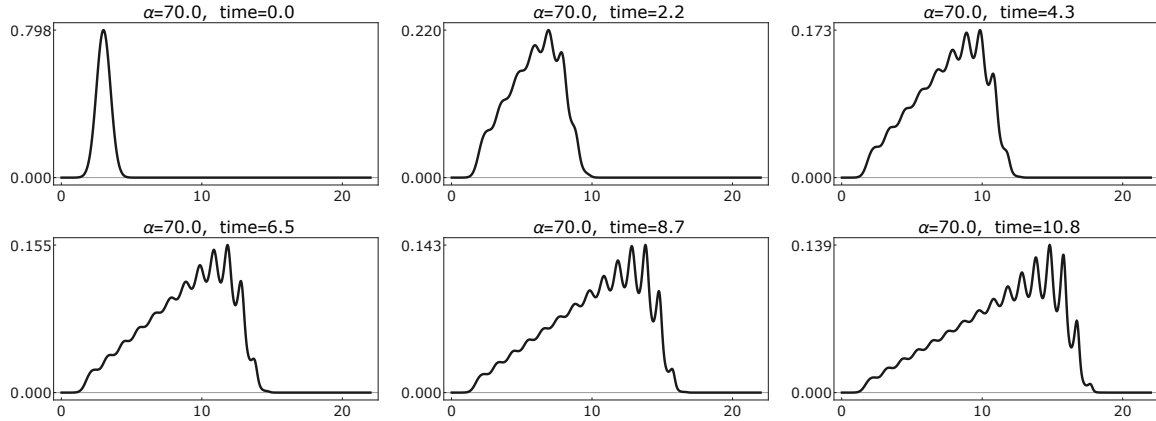


Figure 12: Evolution for smooth integrable initial data for $\alpha = 70$.

4 Summary and concluding remarks

In this article we studied the long-time behaviour of solutions to the coagulation equations for kernels with homogeneity one. For kernels with this homogeneity the long-time behaviour depends on whether the kernel is diagonally dominant (called class-I in the literature) or not. In the latter case one expects that a family of self-similar solutions with finite mass exists and solutions converge to a member of this family which has the same decay behaviour as the initial data. However, to rigorously establish just the existence of such a family and in particular to determine their precise range seems in general a difficult task.

For class-I kernels, no self-similar solutions with finite mass can exist. In suitable variables (see (7) and (8)) heuristics suggest that the long-time behaviour should be as in the classical Burgers equation, which means that for integrable data solutions approximate an N -wave in the limit. We performed numerical simulations that confirm this conjecture, but they also reveal that the details of how the N -wave is approximated is quite unusual. In particular, for kernels that are not close to the diagonal one, we observe strong oscillations near the shock front. Those can be explained by the fact that the transition at the shock is given by traveling wave profiles. A linear analysis indeed suggests that these traveling waves are oscillatory which is also observed in numerical simulations for Riemann data. It would be very interesting to rigorously prove the existence of such traveling waves and understand their regularity and stability properties. In a first step this might be feasible for kernels close to the diagonal one. This case is also of particular interest due to the instability of the constant solutions that we found in this regime and the results of numerical simulations that suggest that also traveling waves are unstable for such kernels.

A Scheme for the numerical simulations

The starting point for numerical simulations is the time-dependent problem (1) in an exponentially rescaled space variable but as in Section 3.2 it is convenient to replace the scaling law (7) by

$$\xi = 2^X, \quad X = \frac{\ln \xi}{\ln 2}, \quad T = t \ln 2, \quad \xi^2 f(t, \xi) = u(t \ln 2, \ln \xi / \ln 2). \quad (54)$$

Moreover, it is also reasonable to normalize the kernel by $\int_0^1 K(x, 1-x) dx = 1$, which implies $c_\alpha = \Gamma(2 + 2\alpha)/\Gamma(1 + \alpha)^2$ for the family (12).

In the diagonal case, the nonlinear lattice equation (26) has a natural interpretation as a hierarchy of time-dependent ODEs, provided that the initial data are constant for $j < j_0$. In fact, $u_j(0) = c$ for all $j < j_0$ implies $u_j(t) = c$ for all $j < j_0$ and $t \geq 0$, and by iteration we can hence regard (26) as a non-autonomous ODE for the output u_j with known input u_{j-1} . This allows us to employ standard scalar ODE integrators, as for instance `DSolve` in `MATHEMATICA`, for the numerical solution of the discrete Burgers lattice (26); cf. Figure 4. For non-diagonal kernels such as (12), the dynamical equation (1) can, thanks to (8) and (54), be written as

$$\partial_T u(T, \cdot) = \mathcal{I}_{\text{gain}}(u(T, \cdot)) - \mathcal{I}_{\text{loss}}(u(T, \cdot)) \quad (55)$$

with

$$\begin{aligned}\mathcal{I}_{\text{gain}}(u(T, \cdot))|_X &:= \int_0^\infty W_{\text{gain}}(Y) u(T, X - 1 - Y) u(T, X - 1 + \hat{Y}(Y)) dY \\ \mathcal{I}_{\text{loss}}(u(T, \cdot))|_X &:= u(T, X) \int_{-\infty}^\infty W_{\text{loss}}(Y) u(T, X - Y) dY.\end{aligned}\tag{56}$$

Here, the weight functions are defined by

$$W_{\text{gain}}(Y) := \frac{K_\alpha(2^{Y+1} - 1, 1)}{(1 - 2^{-1-Y})^2}, \quad W_{\text{loss}}(Y) := K_\alpha(2^{-Y}, 1) 2^Y \tag{57}$$

and the function \hat{Y} with

$$\hat{Y}(Y) := \frac{\ln(2 - 2^{-Y})}{\ln 2} \tag{58}$$

is strictly increasing for $Y > 0$ and satisfies $Y(0) = 0$, $Y(+\infty) = 1$, see Figure 13. As illustrated

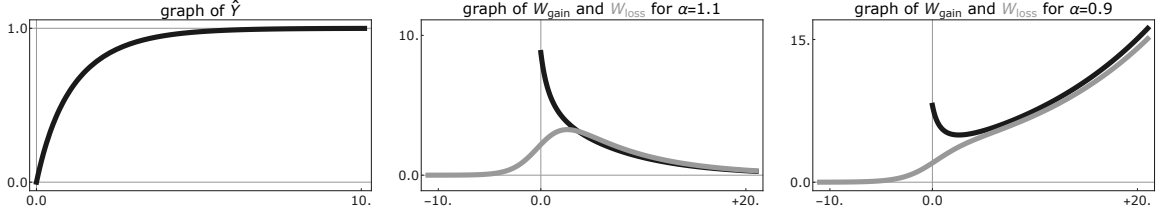


Figure 13: Graph of the function \hat{Y} in (58) as well as typical examples of the moment weights from (57) for the α -kernel (12) with $\alpha > 1$ and $0 < \alpha < 1$.

in Figure 13, the weight functions from (57) can behave rather differently as $Y \rightarrow \infty$ and in the case of non-decaying weight functions it is not advisable to discretize the two integrals in (56) independently of each other. On the contrary, for the kernels in (12) it is more convenient to reformulate (55) as

$$\partial_T u(T, \cdot) = \mathcal{I}_A(u(T, \cdot)) + \mathcal{I}_B(u(T, \cdot)) - \mathcal{I}_C(u(T, \cdot)), \tag{59}$$

where the three integral operators

$$\begin{aligned}\mathcal{I}_A(u(T, \cdot))|_X &:= \int_0^\infty W_{\text{gain}}(Y) u(T, X - 1 - Y) (u(T, X - 1 + \hat{Y}(Y)) - u(T, X)) dY \\ \mathcal{I}_B(u(T, \cdot))|_X &:= u(T, X) \int_0^\infty (W_{\text{gain}}(Y) - W_{\text{loss}}(Y + 1)) u(T, X - 1 - Y) dY \\ \mathcal{I}_C(u(T, \cdot))|_X &:= u(T, X) \int_0^\infty W_{\text{loss}}(1 - Y) u(T, X - 1 + Y) dY,\end{aligned}\tag{60}$$

possess better properties than $\mathcal{I}_{\text{gain}}$ and $\mathcal{I}_{\text{loss}}$. In fact, the weight functions for \mathcal{I}_B and \mathcal{I}_C decay exponentially as $Y \rightarrow \infty$, while the properties of \hat{Y} ensure that $u(T, X - 1 + \hat{Y}(Y)) - u(T, X)$ decays faster than $1/W_{\text{gain}}(Y)$ provided that u is sufficiently regular at (T, X) . All numerical data presented in this paper, see Figures 8, 11, are computed by a MATLAB implementation of the following, straight forward discretization of (59):

1. Compute u on the spatial grid $X \in \varepsilon\mathbb{Z} \cap [0, L]$, where $1 \ll L < \infty$ is a given discretization length and $0 < \varepsilon \ll 1$ a chosen spacing.

2. Continue u constantly for $X < 0$ and $X > L$ by constants c_- and c_+ , respectively, with $c_- = c_+ = 0$ for integrable initial data and $c_- > 0$, $c_+ = 0$ in order to compute traveling waves.
3. Approximate all integrals from (60) by Riemann sums with respect to $Y \in \varepsilon\mathbb{Z} \cap [0, R]$, where $R > 1$ is another discretization parameter.
4. Use the explicit Euler scheme with step size $0 < \tau \ll 1$ for the time integration.

The resulting numerical scheme, however, is neither very accurate nor fast. It remains a challenging task to construct alternative algorithms that allow to resolve the long time behavior of coagulation equations with diagonal dominant kernels of homogeneity 1 more efficiently. In previous work Filbet and Laurençot [8] developed a finite volume scheme to simulate the coagulation equation in the conservative form (2), but did not study the long-time behaviour specifically for kernels with homogeneity one. Lee [12] simulated the discrete version of the coagulation equation. He considered the case of class-I kernels with homogeneity one, but the convergence of the algorithm is slow in this case and the results are not completely conclusive. It seems that no numerical simulations of the coagulation equation have been previously performed for the equation in exponential variables (8). We also mention that the dynamical solutions computed with the traveling wave continuation $u(T, X) = c_- > 0$ and $u(T, X) = c_+ = 0$ for $X < 0$ and $X > L$, respectively, might be unphysical for small times due to artificial boundary effects. For sufficiently large times and sufficiently large computational domains, however, those numerical solutions approach a traveling wave that connects c_- to c_+ .

Acknowledgment. The authors acknowledge support through the CRC 1060 *The mathematics of emergent effects* at the University of Bonn that is funded through the German Science Foundation (DFG).

References

- [1] M. Abramowitz and I. A. Stegun. Handbook of Mathematical Functions with formulas, graphs, and mathematical tables. *National Bureau of Standards Applied Mathematics Series*, 55, 1964.
- [2] D. J. Aldous. Deterministic and stochastic models for coalescence (aggregation and coagulation): a review of the mean-field theory for probabilists. *Bernoulli*, 5(1):3–48, 1999.
- [3] E. Ben-Naim and P. L. Krapivsky. Discrete analogue of the Burgers equation. *J. Phys. A*, 45(45):455003, 9, 2012.
- [4] J. Bertoin. Eternal solutions to Smoluchowski’s coagulation equation with additive kernel and their probabilistic interpretations. *Ann. Appl. Probab.*, 12(2):547–564, 2002.
- [5] M. C. Cross and P. C. Hohenberg. Pattern formation outside of equilibrium. *Rev. Mod. Phys.*, 65(3):851–1112, 1993.
- [6] R.-L. Drake. A general mathematical survey of the coagulation equation. In *Topics in current aerosol research (part 2)*, Hidy G. M., Brock, J. R. eds., International Reviews in Aerosol Physics and Chemistry, pages 203–376. Pergamon Press, Oxford, 1972.
- [7] M. Escobedo, S. Mischler, and M. Rodriguez Ricard. On self-similarity and stationary problem for fragmentation and coagulation models. *Ann. Inst. H. Poincaré Anal. Non Linéaire*, 22(1):99–125, 2005.
- [8] F. Filbet and P. Laurençot. Numerical simulation of the Smoluchowski coagulation equation. *SIAM J. Sci. Computing*, 6:2004-2-28, 2004.

- [9] N. Fournier and P. Laurençot. Existence of self-similar solutions to Smoluchowski's coagulation equation. *Comm. Math. Phys.*, 256(3):589–609, 2005.
- [10] S.K. Friedlander. *Smoke, Dust and Haze: Fundamentals of Aerosol Dynamics*. Topics in Chemical Engineering. Oxford University Press, second edition, 2000.
- [11] L. Ignat, A. Pozo, and E. Zuazua. Large-time asymptotics, vanishing viscosity and numerics for 1-D scalar conservation laws. *Math. Comp.*, 84(294):1633–1662, 2015.
- [12] M. H. Lee. A survey of numerical solutions of the coagulation equation. *J. Phys. A*, 34:10219–10241, 2001.
- [13] E. M. Lifshitz and L. P. Pitaevskii. Landau and Lifshitz: Physical kinetics. *Course of Theoretical Physics, Volume 10*.
- [14] P. Laurençot and S. Mischler. From the discrete to the continuous coagulation-fragmentation equations. *Proc. Roy. Soc. Edinburgh Sect. A*, 132(5):1219–1248, 2002.
- [15] P. Laurençot, B. Niethammer, and J.J.L. Velázquez. Oscillatory dynamics in Smoluchowski's coagulation equation with diagonal kernel. 2016. Preprint, arxiv:1603.02929.
- [16] R. Leyvraz. Scaling theory and exactly solvable models in the kinetics of irreversible aggregation. *Phys. Reports*, 383:95–212, 2003.
- [17] T. P. Liu and M. Pierre. Source-solutions and asymptotic behavior in conservation laws. *J. Differential Equations*, 51(3):419–441, 1984.
- [18] J. B. McLeod, B. Niethammer, and Velázquez J.J.L. Asymptotics of self-similar solutions to coagulation equations with product kernel. *J. Stat. Phys.*, 144:76–100, 2011.
- [19] G. Menon and R. L. Pego. Approach to self-similarity in Smoluchowski's coagulation equations. *Comm. Pure Appl. Math.*, 57(9):1197–1232, 2004.
- [20] B. Niethammer, S. Throm, and J. J. L. Velázquez. A revised proof of uniqueness of self-similar profiles to Smoluchowski's coagulation equation for kernels close to constant. 2015. Preprint, arxiv:1510.03361.
- [21] B. Niethammer, S. Throm, and J. J. L. Velázquez. Self-similar solutions with fat tails for Smoluchowski's coagulation equation with singular kernels. *Ann. Inst. Henri Poincaré (C) Nonlinear Analysis*, 2016. to appear.
- [22] B. Niethammer and J. J. L. Velázquez. Self-similar solutions with fat tails for Smoluchowski's coagulation equation with locally bounded kernels. *Comm. Math. Phys.*, 318:505–532, 2013.
- [23] B. Niethammer and J. J. L. Velázquez. Oscillatory traveling waves for a coagulation equation. 2016. In preparation.
- [24] R. L. Pego, P. Smereka, and M. I. Weinstein. Oscillatory instability of traveling waves for a KdV-Burgers equation. *Phys. D*, 67(1-3):45–65, 1993.
- [25] B. Sandstede and A. Scheel. Absolute versus convective instability of spiral waves. *Phys. Rev. E*, 62(6): 7708–7714, 2000.
- [26] M. Smoluchowski. Drei Vorträge über Diffusion, Brownsche Molekularbewegung und Koagulation von Kolloidteilchen. *Physik. Zeitschrift*, 17:557–599, 1916.
- [27] A. M. Turing. The chemical basis of morphogenesis.. *Philosophical Transactions of the Royal Society of London, Series B, Biological Sciences.*, 237:37–72, 1952.
- [28] P. G. J. van Dongen and M. H. Ernst. Scaling solutions of Smoluchowski's coagulation equation. *J. Statist. Phys.*, 50(1-2):295–329, 1988.